insects

MDPI

Article

A Self-Regulatory Viral Small RNA Embedded in the Promoter Region of a Novel Transcript Facilitates Bombyx mori Bidensovirus Replication

Qian Yu *, Yuting Zhuang, Zhimin Xiong, Jiaxin Yan, Feifei Zhu, Lindan Sun, Shangshang Ma, Xiaoyong Liu and Qi Tang *

School of Biological Science and Technology, Jiangsu University, Zhenjiang 212013, China; yutingzhuang0627@163.com (Y.Z.); 18183811145@163.com (Z.X.); yanjiaxin9899@163.com (J.Y.); feifzhu@ujs.edu.cn (F.Z.); sunlindan@ujs.edu.cn (L.S.); mashang@ujs.edu.cn (S.M.); liuxiaoyong@ujs.edu.cn (X.L.)
* Correspondence: qianyu@ujs.edu.cn (Q.Y.); tangqi1224@163.com (Q.T.); Tel.: +86-150-5085-3270 (Q.Y.)

Simple Summary

The silkworm, *Bombyx mori*, is an economically important insect, but silkworm rearing is threatened by viral diseases, including infection by Bombyx mori bidensovirus (BmBDV). Viruses can produce tiny regulatory molecules called small RNAs, which may help them control their own genes. In this study, we analyzed all RNAs present in the silkworm midgut after BmBDV infection and discovered (i) a previously unknown viral transcript, named transcript IV, and (ii) a highly abundant viral small RNA, vsRNA-18895, which is produced from a short region shared by several viral genes; a complementary small RNA of nearly similar abundance was also detected from this region. When we injected silkworms with a double-stranded RNA corresponding to vsRNA-18895 (an agomir), the virus copied its genome more efficiently and produced more of the RNAs needed for replication; when we injected a single-strand RNA complementary to vsRNA-18895 (an antagomir), replication decreased. Our results are consistent with BmBDV using this small RNA, possibly together with a complementary antisense species of similar abundance, to boost its own replication through a positive feedback loop, although whether the sense strand alone is responsible remains to be shown. This small RNA may serve as a marker of infection and as a target for new strategies to protect silkworms from viral disease.

Abstract

Bombyx mori bidensovirus (BmBDV) is a bipartite single-stranded DNA virus that causes severe losses in sericulture, yet its transcriptional complexity and possible self-regulatory viral small RNAs remain unexplored. Here, transcriptome and small RNA sequencing of BmBDV-infected midguts was performed to identify novel viral transcripts and functional virus-derived small RNAs (vsRNAs). A previously unrecognized transcript (transcript IV, nt 290–2929) was discovered on the VD1 segment, sharing its 5′ promoter region with NS2 and its 3′ polyadenylation signal with VP. Notably, the most abundant viral small RNA, a 20-nt vsRNA designated vsRNA-18895 (TPM up to 11,750), mapped to the promoter-overlap region shared by NS1, NS2 and transcript IV (VD1 nt 596–615). In vivo agomir/antagomir experiments showed that injection of a double-stranded RNA corresponding to vsRNA-18895 (an agomir) significantly upregulated NS1, NS2 and transcript IV (up to 103.52-, 102.47- and 101.87-fold, respectively) and enhanced VD1 replication (103.26-fold), whereas injection of a single-strand RNA complementary to vsRNA-18895 (an antagomir) suppressed them; VD2 and other viral genes (VP, PolB, NS3 and P133) were unaffected.

Check for updates

Academic Editor: Jeff Wilusz

Received: 17 September 2026
Revised: 19 October 2026
Accepted: 22 October 2026
Published: 27 October 2026

Copyright: © 2026 by the authors. Licensee MDPI, Basel, Switzerland. This article is an open access article distributed under the terms and conditions of the Creative Commons Attribution (CC BY) license.

Because the abundance of vsRNA-18895 itself was not directly measured following antagomir injection, this treatment may either reduce, or merely interfere with, the activity of the small RNA. These findings are consistent with a positive feedback loop in which a virus-encoded small RNA embedded in the promoter region of a novel transcript facilitates BmBDV replication, providing functional evidence of a self-regulatory vsRNA in an invertebrate single-stranded DNA virus. Because a complementary antisense small RNA produced from the same locus was of comparable abundance, a possible contribution of that strand to the observed effects cannot be excluded.

Keywords: Bombyx mori bidensovirus; virus-derived small RNA (vsRNA); transcript IV; positive feedback regulation; viral replication

1. Introduction

The domesticated silkworm, *Bombyx mori*, has been cultivated for more than five thousand years and remains an insect of considerable economic, cultural and scientific importance in many Asian countries [1]. However, sustainable sericulture is continually threatened by viral diseases, including cytoplasmic polyhedrosis virus (CPV), Bombyx mori nucleopolyhedrovirus (BmNPV) and Bombyx mori bidensovirus (BmBDV; family Bidnaviridae) [2,3]. Among these, BmBDV is the aetiological agent of infectious flacherie of silkworm larvae and is widely regarded as one of the most damaging silkworm pathogens in China, where infected batches typically display larval atrophy, delayed development, and high mortality [4,5]. BmBDV is a non-enveloped icosahedral virus whose capsid packages two linear single-stranded DNA segments, namely VD1 (~6500 nucleotides) and VD2 (~6000 nucleotides), both of which are required for productive infection [6,7].

On a single (plus) strand, the VD1 segment encodes the non-structural proteins NS1 and NS2 and the structural capsid protein VP. NS1 contains Walker A/B helicase motifs and binds the viral origin of replication, whereas NS2 shares homology with bacterial DnaA-like replication-initiation factors and accumulates at the host nuclear membrane [6,8]. The VD2 segment encodes the DNA polymerase B (PolB) and two additional proteins of as-yet-undefined function, NS3 and P133 [7,9]. By combining RACE, Northern blotting and quantitative PCR, our group and others previously established a provisional transcription map of BmBDV in which each ORF is expressed as a discrete mRNA [9,10]. Nevertheless, the structural completeness and the inter-relationships of BmBDV transcripts are not yet fully resolved, and earlier low-resolution analyses may have missed rare or spatially restricted isoforms [11].

In parallel with protein-coding transcripts, viruses across diverse kingdoms produce virus-encoded small RNAs (vsRNAs) during the infection cycle. Prominent examples include the miRNAs of herpesviruses such as HSV-1, EBV and KSHV that modulate latency and host-immune gene expression [12–14], and the siRNA-class vsRNAs generated from many plant and animal RNA viruses that direct the host RNAi machinery against viral transcripts [14,15]. In the insect virome, vsRNAs have been reported from several parvoviruses, dicistroviruses and reoviruses; they often map to discrete hotspots in the viral genome and in some cases have been shown to regulate viral replication and host antiviral defence [16–19]. Notably, in the planthopper dicistrovirus system, vsRNAs accumulate predominantly as ~20-nucleotide species derived from both strands, raising the possibility that small RNAs may be used to fine-tune viral gene expression in insect hosts [18]. Whether a comparable vsRNA-based regulatory layer exists in any lepidopteran parvovirus, and specifically in BmBDV, has remained unknown.

The silkworm relies on a robust RNA interference (RNAi) pathway as its principal antiviral defence mechanism, and experimental disruption of Dicer-2, Argonaute-2 or related components markedly increases susceptibility to BmNPV, BmCPV and several other silkworm viruses [20–22]. It is therefore plausible that BmBDV infection triggers the production of vsRNAs processed by the host RNAi machinery, and that at least some of these vsRNAs are more than mere by-products of host defence; they may in fact participate in regulating viral gene expression, conceptually analogous to miRNA-mediated regulation of host mRNAs [14,23]. An emerging body of work in plant and insect viruses has proposed that virus-encoded small RNAs can serve in cis and in trans as regulators of viral transcription, although concrete mechanistic evidence for such regulation in insect parvoviruses has remained scarce [15,19,24].

In the present work, we sought to address four questions in the B. mori–BmBDV system: (i) is the BmBDV transcription map more complex than previously appreciated; (ii) does BmBDV infection produce a discrete vsRNA population that can be systematically catalogued; (iii) does the most abundant vsRNA originate from a specific genomic locus, in particular the 5′-shared region of NS1 and NS2; and (iv) does that vsRNA exert a sequence-specific regulatory effect on viral gene expression and viral replication in vivo? To this end, we performed poly(A)-RNA sequencing and small RNA sequencing on BmBDV-infected fifth-instar B. mori midgut tissue at 72 h post-inoculation (hpi). This yielded a refined BmBDV transcription map that includes a previously unannotated, NS-VP-spanning transcript of VD1, tentatively designated transcript IV, and identified a small RNA landscape dominated by a 20-nt species termed vsRNA-18895 (TPM = 11,750) that maps precisely within positions 596–615 of VD1—within the 5′-shared segment of NS1, NS2 and transcript IV. Using chemically synthesised agomir and antagomir reagents delivered by intracoelomic injection into BmBDV-inoculated larvae, we show that modulation of the 596–615 small-RNA locus selectively and positively affects the expression of NS1, NS2 and transcript IV without affecting the VP, PolB, NS3 or P133 transcripts, and is associated with a specific increase in the replication of the VD1 segment. Together, our results are consistent with a virus-encoded small-RNA-mediated positive feedback loop that coordinates non-structural gene expression with viral genome replication in BmBDV, and point to a new layer of small-RNA-based cis-regulation in a lepidopteran parvovirus.

2. Materials and Methods

2.1. Silkworm Rearing, Virus Inoculation and Midgut Sampling

Larvae of the BmBDV-susceptible silkworm strain ‘Jingsong × Haoyue’, maintained at the School of Life Sciences, Jiangsu University, were used throughout this study. Eggs were hatched and larvae were reared on fresh mulberry leaves coated with antibiotics under controlled conditions of 26 °C, 60% relative humidity and a 12 h light/12 h dark photoperiod until the fifth instar. To prepare the viral inoculum, 0.5 g of BmBDV-infected larval midgut powder stored at 4 °C was homogenised in 5 mL of sterile water; the homogenate was centrifuged at 12,000× *g* for 15 min at 4 °C, and the supernatant was incubated with an equal volume of 0.2 M acetic acid for 40 min at room temperature to inactivate contaminating microorganisms. The pH was adjusted to 7.0 with 1% Na_2CO_3, and the suspension was brought to a final concentration of 20 mg/mL (midgut wet-weight equivalent) with sterile water and stored at 4 °C until use. Newly ecdysed fifth-instar larvae were orally inoculated with 5 µL of the viral suspension per larva by droplet feeding. Mock-inoculated control larvae were handled identically but received an equal volume (5 µL per larva) of sterile water instead of the viral suspension. For the infection time course, midguts were dissected under sterile conditions at 24, 48 and 72 h post-inoculation (hpi), rinsed with ice-cold phosphate-buffered saline (PBS) to remove mulberry-leaf debris,

and transferred to RNAlater (Thermo Fisher Scientific, Waltham, MA, USA) in RNase-free tubes. Three midgut tissue samples were collected per time point as biological replicates and stored at −80 °C until RNA or DNA extraction.

2.2. Total RNA Extraction and cDNA Synthesis

All surfaces and instruments were treated with an RNase decontamination solution, and forceps were soaked in 0.1% DEPC-treated water; all plasticware was RNase-free. Total RNA was extracted from midgut tissue using TRIzol reagent (Invitrogen, Thermo Fisher Scientific, Waltham, MA, USA) according to the manufacturer's instructions. Briefly, a frozen midgut sample was homogenised in pre-cooled TRIzol with a hand-held homogeniser and processed through phase separation, RNA precipitation, washing and dissolution. RNA concentration and purity were measured with a OneDrop spectrophotometer (Nanjing Wuyi Technology Co., Ltd., Nanjing, China) (or equivalent), and RNA integrity was verified when required (A260/A280 = 1.8–2.2). Aliquots were stored at −80 °C. Genomic DNA contamination was removed by DNase I digestion before reverse transcription. First-strand cDNA was synthesised from 1 μg of total RNA with a commercial reverse-transcription kit following the manufacturer's protocol (reverse transcription at 42 °C for 30 min, heat inactivation at 85 °C for 5 s).

2.3. Transcriptome Sequencing, Assembly and Prediction of Novel Transcripts

Viral transcriptome sequencing was performed by Shanghai Ouyi Medical Technology Biotechnology Co., Ltd. Total RNA was extracted with TRIzol from midgut tissue of six fifth-instar larvae (three BmBDV-inoculated and three mock-inoculated controls) collected at 72 hpi and treated with DNase I. RNA quality and integrity were assessed with a NanoDrop spectrophotometer (Thermo Fisher Scientific, Waltham, MA, USA) and an Agilent 2100 Bioanalyzer (Agilent Technologies, Santa Clara, CA, USA). Poly(A) mRNA was captured with oligo(dT) magnetic beads, and sequencing libraries were constructed with the NEBNext Ultra RNA Library Prep Kit (New England Biolabs, Ipswich, MA, USA), including first- and second-strand cDNA synthesis, end repair, A-tailing, adapter ligation and PCR enrichment of 300–500 bp fragments. Libraries were sequenced on an Illumina NovaSeq 6000 platform as 150 bp paired-end reads. Raw reads were quality-checked with FastQC [25] and trimmed with Trimmomatic [26] to obtain clean reads. Clean reads were aligned to the BmBDV reference genome with STAR [27]; reads that failed to map to annotated regions, together with reads mapping to intergenic regions, were assembled de novo with StringTie [28] to construct candidate transcript models. Open reading frames (ORFs) of the candidate transcripts were predicted with TransDecoder [29], and candidates with complete ORFs (≥100 aa) were retained. Transcript abundance was estimated with RSEM [30]. Newly assembled transcripts were compared against the NCBI non-redundant nucleotide database by BLAST (National Center for Biotechnology Information, https://www.ncbi.nlm.nih.gov/blast/, accessed on 26 October 2022); sequences with <95% identity and <80% coverage to any known transcript were classified as potential novel transcripts and subjected to functional annotation with eggNOG-mapper and the Pfam database. All six libraries were sequenced and the raw data have been deposited in the NCBI SRA under BioProject PRJNA1529325; the analyses described below were performed on the three BmBDV-inoculated libraries.

2.4. RACE Validation of Viral Transcript Termini

The transcription start site (TSS) and transcription termination site (TTS) of the novel transcript IV were determined by rapid amplification of cDNA ends (RACE) using the SMARTer® RACE 5′/3′ Kit (Takara Bio, Shiga, Japan). Where required, poly(A) mRNA was first purified from total RNA by magnetic separation with VAHTS mRNA Capture Beads

2.0 (Vazyme, Nanjing, China). For 5′-RACE, a gene-specific primer (GSP) annealing near the 5′ end of the target mRNA was used to prime first-strand cDNA synthesis; the template-switching activity of the reverse transcriptase added non-templated nucleotides that allowed extension from the SMARTer II A oligonucleotide, and the 5′ end was subsequently amplified by RACE-PCR with the GSP and a universal primer. For 3′-RACE, an oligo(dT) primer was used to prime first-strand cDNA synthesis from the poly(A) tail, and the 3′ end was amplified with a GSP and a universal primer. RACE-PCR products were resolved by 1% agarose gel electrophoresis, and bands of the expected size were excised, purified with a gel-extraction kit, ligated into the pMD18-T/pMD19-T vector (Takara Bio) at 16 °C overnight and transformed into Escherichia coli DH5α-competent cells. Positive clones were verified by colony PCR, and plasmid inserts were sequenced by Sanger sequencing to map the precise transcript termini on the BmBDV genome. Primer sequences are listed in Table S2.

2.5. Absolute RT-qPCR Quantification of Viral Transcripts

Absolute standard curves were generated from ten-fold serial dilutions (10^3–10^9 copies/μL) of plasmids carrying each target region; plasmid copy numbers were calculated from spectrophotometric concentrations, and Ct values were regressed against the natural logarithm of copy number (standard curve $y = a \cdot \ln(x) + b$; $R^2 > 0.99$). RT-qPCR was performed with a SYBR Green-based kit, each 20-μL reaction containing SYBR Green master mix, a transcript-specific primer pair (Table S2) and cDNA template. Amplification proceeded as follows: 95 °C for 30 s; 40 cycles of 95 °C for 10 s and 60 °C for 30 s; and a final melting-curve step of 95 °C for 15 s, 60 °C for 1 min, 95 °C for 15 s. Each sample was analysed in triplicate with a no-template control, and product specificity was confirmed by melting-curve analysis. Ct values were converted to absolute copy numbers per μL by interpolation on the corresponding standard curve. In the agomir/antagomir experiments, transcript levels were normalised to the scrambled negative-control (NC) group at each time point (set to 1).

2.6. Small RNA Library Construction, Sequencing and vsRNA Identification

Small RNA sequencing was performed by Shanghai Ouyi Medical Technology Biotechnology Co., Ltd. using midgut tissue collected at 72 hpi from the same three BmBDV-inoculated larvae used for transcriptome sequencing. Total RNA was extracted and quality-assessed as described in Section 2.2. Small RNA fragments of 18–30 nt were recovered after electrophoretic separation of total RNA, ligated to 5′ and 3′ adapters, reverse-transcribed and PCR-amplified; the 140–160 bp products were gel-purified to obtain the small RNA library. Libraries that passed quality control were sequenced on an Illumina NovaSeq 6000 platform (single-end 50 bp). Raw reads were filtered to retain sequences of 15–41 bp, and adapter sequences, low-quality reads and contaminating sequences were removed to obtain clean reads. Clean reads were aligned to the BmBDV reference genome (VD1 and VD2 segments) with Bowtie [31], allowing no more than one mismatch, and reads that mapped uniquely to the viral genome were defined as virus-derived small RNAs (vsRNAs). The length distribution, strand specificity, read abundance and genomic coordinates of vsRNAs were determined from the alignment. Abundance was normalised and expressed as transcripts per million (TPM) for ranking of individual vsRNA species. The small RNA sequencing data have been deposited in the NCBI SRA under BioProject PRJNA1529325.

2.7. Agomir/Antagomir Design and In Vivo Injection

To modulate the abundance of vsRNA-18895 in vivo, a chemically synthesised agomir mimicking vsRNA-18895 (sense strand 5′-GAAAAGGCUGACGAUCUCCU-3′ and its complementary strand) and a specific antagomir (5′-AGGAGAUCGUCAGCCUUUUC-3′) were

designed, together with a scrambled non-targeting RNA as the negative control (NC); sequences are listed in Table S2. Because no BmBDV-permissive cell line is available and the virus requires an entry window, larvae were first infected and the reagents were delivered after the infection was established. Specifically, 240 newly ecdysed fifth-instar larvae were orally inoculated with the BmBDV suspension (5 μL/larva); at 8 hpi, larvae were randomly allocated to four groups: (i) vsRNA-18895 agomir plus BmBDV (agomir + BmBDV); (ii) antagomir plus BmBDV (antagomir + BmBDV); (iii) NC RNA plus BmBDV (NC + BmBDV); and (iv) BmBDV alone. Agomir, antagomir and NC were injected intracoelomically at 2 μg per larva. To prevent secondary infection caused by the injection procedure, mulberry leaves were sprayed with 0.1% norfloxacin solution and fed to the larvae for 24 h after injection, after which routine rearing was resumed. Midguts were collected at 24, 48, 72 and 96 h post-injection (corresponding to 32, 56, 80 and 104 hpi); at each time point, three larvae were randomly sampled, each larva constituting one biological replicate (n = 3). Midgut tissues were transferred to RNAlater and stored at −80 °C.

2.8. Viral Genomic DNA Extraction and qPCR Quantification of VD1/VD2

Midgut samples collected at each time point were homogenised in a sterile mortar. To remove host nucleic acids, the homogenate was incubated with 10 μL of DNase I and RNase A for 30 min at 37 °C, conditions under which viral DNA remains protected by the capsid. Proteinase K digestion was then performed by mixing 20 μL of Proteinase K with 200 μL of BB5 buffer (supplied with the DNA purification kit) in a sterile 1.5 mL tube, adding 200 μL of the homogenate and incubating at 56 °C for 15 min to release viral DNA from the capsids. After addition of 250 μL of ice-cold absolute ethanol and gentle mixing, the mixture was loaded onto a DNA purification column and processed by centrifugation (12,000× *g*, 1 min), followed by two washes with 500 μL of WB5 buffer, a drying spin and elution in 20–50 μL of RNase-free water. Purified viral DNA was stored at −20 °C. VD1 and VD2 genomic copies were quantified by SYBR Green-based qPCR using standard curves generated from serial dilutions of pVD1 and pVD2 plasmids [32] under the thermal-cycling conditions described in Section 2.5.

2.9. Statistical Analysis

Data were organised in Microsoft Excel and analysed with SPSS (26.0). For time-course and treatment comparisons, one-way analysis of variance (ANOVA) was first performed to test overall differences, followed by Dunnett's multiple-comparison test to evaluate differences between treatment groups and the corresponding control group. A p value < 0.05 was considered statistically significant (*), <0.01 highly significant (**) and <0.001 extremely significant (***); $p > 0.05$ was considered not significant (NS). All experiments were performed with three biological replicates, and results are presented as the mean ± SD unless otherwise stated.

3. Results

3.1. BmBDV Establishes a Robust Infection in the Midgut of Fifth-Instar Bombyx mori Larvae

To establish a reproducible infection system for studying BmBDV–host interactions, fourth-instar molting *Bombyx mori* larvae of the susceptible strain 'Jingsong × Haoyue' were reared under standard conditions and orally inoculated with BmBDV at the onset of the fifth instar. The course of infection was monitored at 24, 48, and 72 h post-inoculation (hpi). Infected larvae displayed no overt behavioural abnormalities at 24 hpi, but feeding activity gradually decreased between 48 and 72 hpi, and the midgut became visibly hypertrophic and pale at 72 hpi, consistent with the characteristic pathology of densovirus infection in lepidopteran larvae. Absolute quantification of the two viral genome segments (VD1

and VD2) by SYBR Green-based qPCR, using the standard curves generated from serial dilutions of plasmids pVD1 ($y = -1.448 \ln(x) + 37.811$, $R^2 = 0.9983$) and pVD2 ($y = -1.480 \ln(x) + 36.687$, $R^2 = 0.9995$), showed that both VD1 and VD2 copy numbers increased in a time-dependent manner in the midgut, reaching peak levels at 72 hpi. The VD1/VD2 standard curves and representative amplification plots are provided in Figure S1. Based on this kinetics profile, 72 hpi midgut tissue was used for all downstream transcriptomic and small RNA sequencing analyses.

3.2. RNA-Seq Identifies a Novel BmBDV Transcript Spanning Both the NS and VP Loci of the VD1 Segment

Poly(A) RNA sequencing was performed on six libraries prepared from 72 hpi midgut tissue of six fifth-instar larvae (three BmBDV-inoculated and three mock-inoculated controls). The three BmBDV-inoculated libraries yielded 50.44–51.22 million raw reads per library; the three mock-inoculated libraries were sequenced in parallel and are publicly available but were not used in the analyses reported here. After quality filtering, 49.43–50.21 million clean reads were retained, with Q30 scores of 93.96–94.07% and an average GC content of 45.37% (Table 1). Per-library sequencing statistics for all six transcriptome libraries, including the three mock-inoculated libraries, are provided in Table S3. Mapping of clean reads against the BmBDV reference genome revealed an average alignment rate of 98.52%, indicating that, by 72 hpi, viral transcripts dominated the poly(A) RNA pool of infected midguts. Annotation against the six previously annotated BmBDV open reading frames (NS1, NS2, VP, PolB, NS3, P133) recovered the corresponding six known transcripts and, in addition, an unannotated isoform that mapped contiguously from the 5′ region of NS1/NS2 to the 3′ region of VP and that was supported by 97.68% of reads in this region (Table 1). This unannotated isoform, hereafter termed "transcript IV", was reproducibly detected across all three biological replicates.

Table 1. Summary of transcriptome sequencing, read quality and mapping to the BmBDV reference genome in the three BmBDV-inoculated libraries from 72 hpi midguts.

Metric	Value (n = 3 BmBDV-Inoculated Libraries)
Raw reads per library (million)	50.44–51.22
Clean reads per library (million)	49.43–50.21
Q30 (%)	93.96–94.07
Average GC content (%)	45.37
Clean reads mapped to the BmBDV genome (%)	98.52 (mean)
Reads supporting transcript IV (%)	97.68

Note: sequencing was performed on six transcriptome libraries in total (three BmBDV-inoculated and three mock-inoculated); the values shown here are for the three BmBDV-inoculated libraries, which were used for all transcriptome analyses reported in this study. Per-library values should be replaced by the exact figures from the sequencing report if the journal requires them.

To independently verify the existence of transcript IV, total RNA was extracted from midguts at 72 hpi and reverse-transcribed. RT-PCR using transcript-specific primer pairs amplified single products of the expected sizes for each of the six known transcripts and, importantly, also for transcript IV, confirming its robust expression at 72 hpi (Figure 1A). To delineate the termini of transcript IV, we performed 5′- and 3′-RACE. Both RACE products (1664 bp for 5′-RACE and 1568 bp for 3′-RACE) were of the expected sizes (Figure 1B) and Sanger sequencing mapped the transcription start site (TSS) of transcript IV to nucleotide position 290 of VD1 and the transcription termination site (TES) to position 2929 of VD1

(Figure 1C,D). Full RACE gels and chromatograms from three independent clones are provided in Figure S3. The 5′-end of transcript IV was thus located within the TATA-box of the NS1 promoter, identical in position to the TSS of NS2, whereas the 3′-end shared a canonical polyadenylation signal (AAUAAA) with the VP transcript. The full-length 2640-nt body of transcript IV thereby spans the junction between the non-structural and structural loci, covering the 89-nt region in which the 3′ ends of the NS1 and NS2 transcripts overlap the 5′ end of the VP transcript.

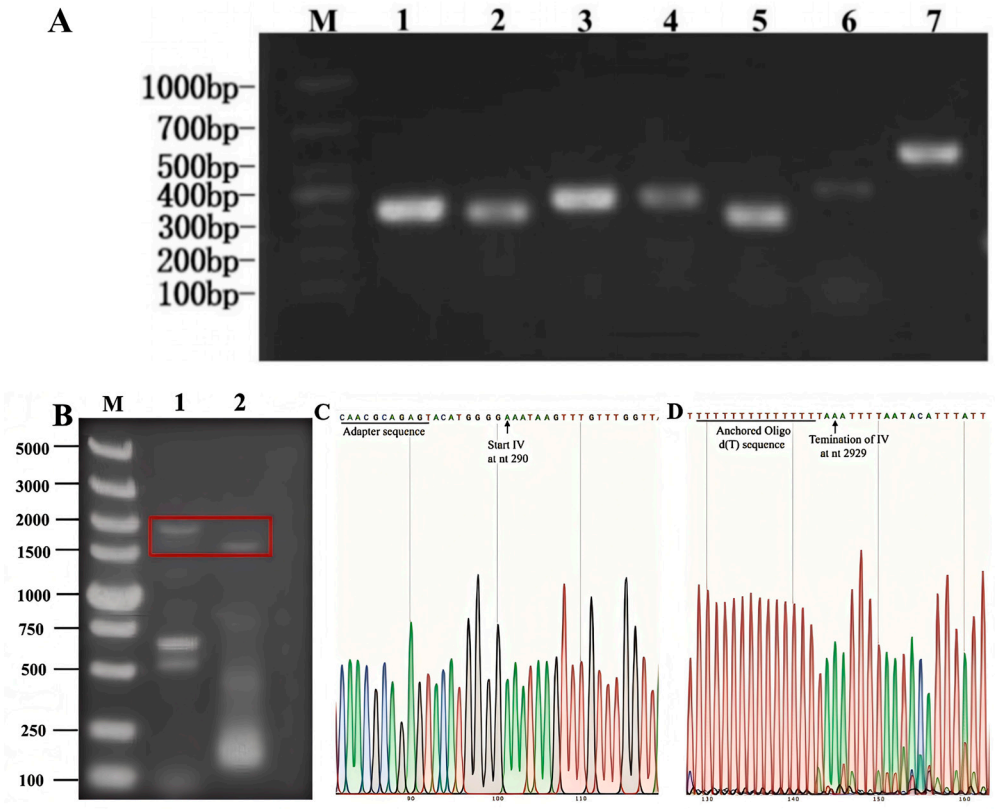


Figure 1. Identification of the novel BmBDV transcript IV. (**A**) RT-PCR verification of all six known transcripts and the novel transcript IV in 72 hpi midgut RNA. Lane M: 1 kb marker; Lanes 1–7: NS1, NS2, VP, PolB, NS3, P133, and IV, respectively. (**B**) 5′-RACE (1664 bp) and 3′-RACE (1568 bp) products. Lane M: 5 kb marker. (**C**) Sanger trace mapping the TSS of transcript IV to VD1 position 290 within the NS1 promoter TATA-box. (**D**) Sanger trace mapping the TES of transcript IV to VD1 position 2929 at the shared VP polyadenylation signal.

The temporal abundance of each viral transcript was then determined by absolute RT-qPCR using transcript-specific primer pairs and standard curves with linearity $R^2 > 0.99$ over a 10^3–10^9 copies/μL range. In the VD1 segment, transcripts NS1, NS2, VP, PolB, and IV were detected at 24, 48, and 72 hpi. Notably, transcript IV was present at the lowest copy number among the VD1-derived transcripts at all time points ($10^{3.09}$ copies/μL at 24 hpi; significantly lower than NS1, NS2, and VP, $p < 0.05$), but its abundance increased progressively with time. In the VD2 segment, NS3 and P133 were both detectable at all time points with NS3 significantly more abundant than P133 ($p < 0.001$). Together, these data refine the BmBDV transcription map by adding transcript IV as a quantitatively minor but consistently expressed NS–VP-spanning isoform on the VD1 segment (Figure 2C,D).

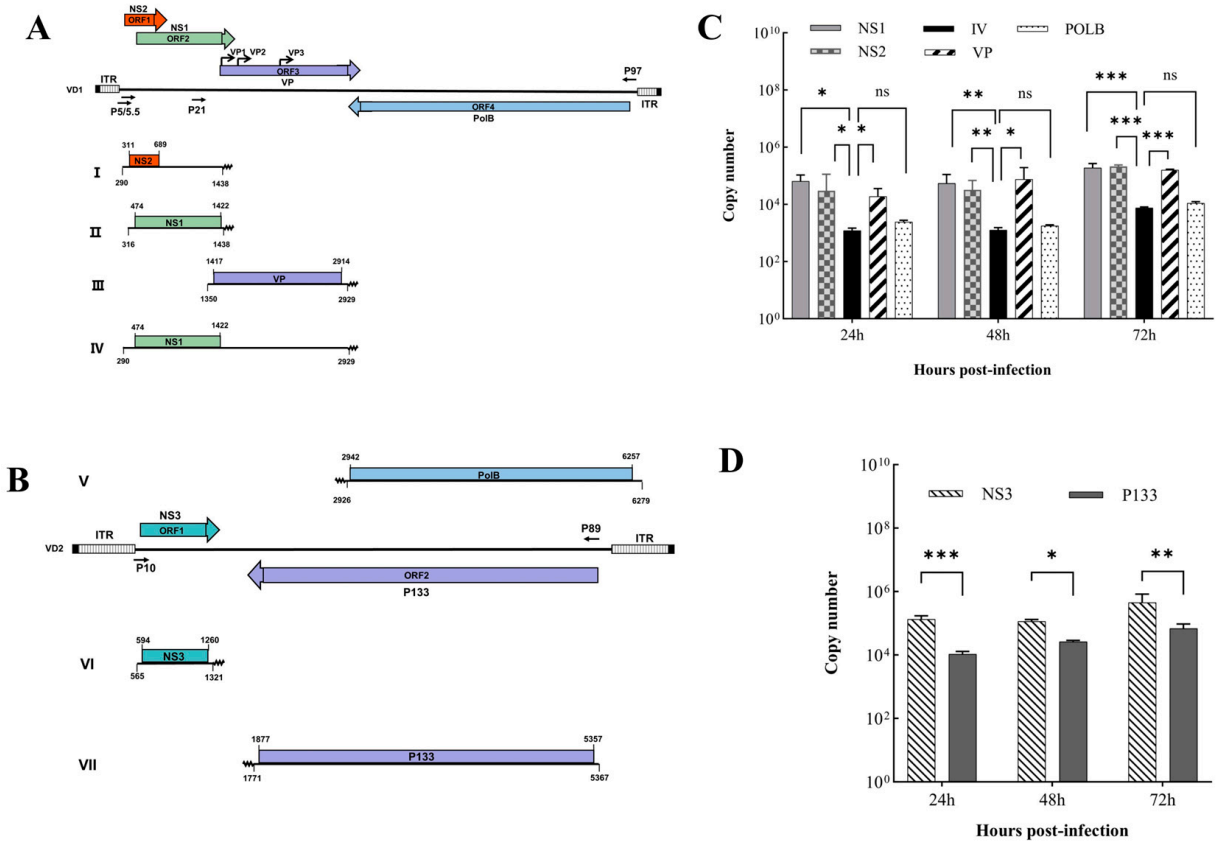


Figure 2. Refined BmBDV transcription map and quantitative abundance of viral transcripts. (**A**,**B**) Refined transcription maps of VD1 (**A**) and VD2 (**B**) showing transcript IV spanning from position 290 to 2929 of VD1; shared TSS with NS2 within the NS1 promoter TATA-box; shared TES and polyadenylation signal with VP; 89-nt overlap between the NS1/NS2 transcript 3′ ends and the VP transcript 5′ end. (**C**) Absolute quantification of NS1, NS2, VP, PolB and IV transcripts in the midgut at 24, 48 and 72 hpi. (**D**) Absolute quantification of NS3 and P133 transcripts in the midgut at 24, 48 and 72 hpi. Dunnett's multiple comparison test; * $p < 0.05$, ** $p < 0.01$, *** $p < 0.001$, ns $p > 0.05$.

3.3. Viral Small RNA Sequencing Identifies a Dominant vsRNA Mapped Within the Shared 5′ Region of NS1, NS2, and Transcript IV

To characterise virus-derived small RNAs (vsRNAs) in BmBDV-infected midguts, total RNA extracted from the midguts of the three BmBDV-inoculated larvae at 72 hpi was used to construct three independent small RNA libraries (15–41 nt) that were sequenced on an Illumina NovaSeq 6000 platform. Each library yielded 23.29–25.85 million raw reads and, after adapter trimming, length filtering (15–41 nt) and quality filtering, 20.81–22.39 million clean reads were retained (Table 2). Per-library statistics for the three small RNA libraries are also provided in Table S3. Bowtie alignment of clean reads against the BmBDV VD1/VD2 reference identified 18,061–28,686 viral reads per library (corresponding to a total of 22,048 viral small RNAs after pooling). The length distribution of these vsRNAs was strongly skewed toward 20–25 nt (~48% of all reads), and within the vsRNA population itself more than 45% of reads were exactly 20 nt in length, suggesting processing by a Dicer-like enzyme. The length distribution of the vsRNA population is provided in Figure S2; strand-specific coverage across the BmBDV genome is shown in Figure 3A.

Table 2. Summary of small RNA sequencing and viral small RNA (vsRNA) recovery in the three BmBDV-inoculated libraries from 72 hpi midguts.

Metric	Value (n = 3 BmBDV-Inoculated Libraries)
Raw reads per library (million)	23.29–25.85
Clean reads per library (million)	20.81–22.39
Reads mapped to the BmBDV genome (per library)	18,061–28,686
Total vsRNAs detected (three libraries pooled)	22,048
Proportion of vsRNA reads 20–25 nt (%)	~48
Proportion of vsRNA reads of exactly 20 nt (%)	>45

Note: three small RNA libraries were constructed from the same three BmBDV-inoculated larvae. Per-library values should be replaced by the exact figures from the sequencing report if the journal requires them.

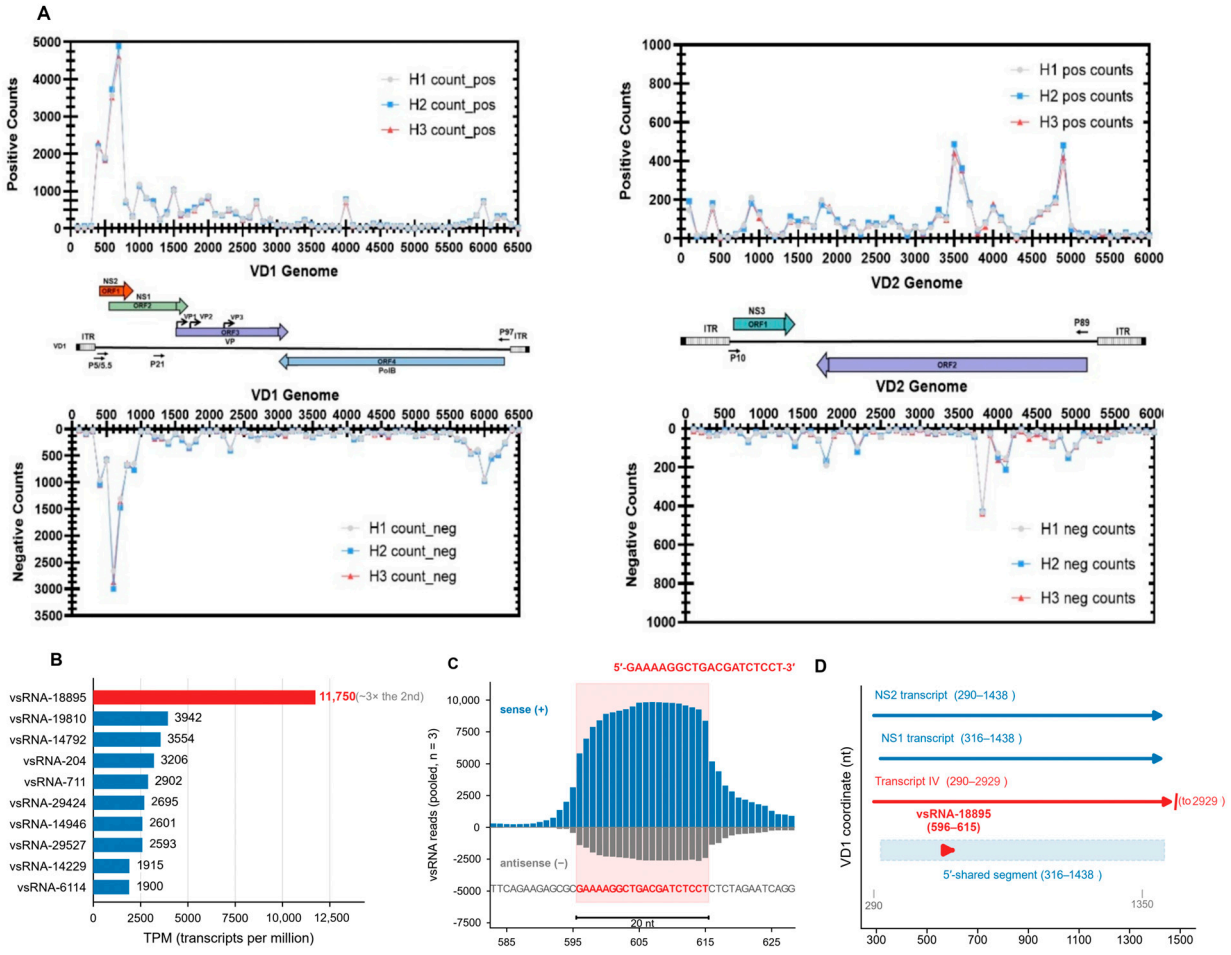


Figure 3. Viral small RNA profiling in BmBDV-infected midgut. (**A**) Genome-wide mapping of vsRNAs onto the BmBDV VD1 and VD2 segments. The y-axes indicate reads count on the sense (above) and antisense (below) strands. ORFs are colour-coded. Note the concentration of vsRNAs in the 5′ region of NS1/NS2/IV. (**B**) Top 10 vsRNAs ranked by TPM. vsRNA-18895 (20 nt) is the dominant species. (**C**) Zoom-in view of the vsRNA cluster mapping within positions 596–615 of VD1, embedded in the NS1/NS2/IV 5′-shared region. (**D**) Schematic showing the vsRNA-18895 cluster within the NS1/NS2/IV-shared 5′ region of transcript IV.

To determine the genomic origin of vsRNAs, the reads were mapped onto the annotated BmBDV genome. The vsRNA reads were distributed across both strands of VD1 and VD2 but with a clear concentration in the 5′-proximal region of the NS1/NS2 locus (Figure 3A). Ranking the vsRNAs by abundance normalised to TPM (transcripts per million) revealed a

strongly dominant species, vsRNA-18895, with a TPM of 11,750, nearly three-fold higher than the second most abundant vsRNA (Figure 3B; Table S1). vsRNA-18895 is 20 nt in length and is precisely encoded at nucleotide positions 596–615 of VD1 (Figure 3C). Critically, positions 596–615 of VD1 lie within the 5′-shared segment of NS1, NS2 and transcript IV (i.e., within the region of VD1 from nt 316 to 1438 that is shared by all three transcripts and internal to both the NS1 and NS2 ORFs), whereas the VP, PolB, NS3, and P133 transcripts do not cover this segment. Three additional highly abundant vsRNAs (vsRNA-14792, vsRNA-204 and vsRNA-711) mapped to immediately adjacent, overlapping positions with highly similar sequences (consensus: 5′-GAAAAGGCTGACGATCTCCT-3′), indicating that this region is a vsRNA hotspot processed from the NS1/NS2/IV-shared 5′ segment. A second, less abundant vsRNA cluster—including vsRNA-19810, vsRNA-14229, vsRNA-14946 and vsRNA-29424—mapped approximately 200 nt upstream (VD1 nt 383–413), also within the NS1/NS2/IV-shared region (Table S1).

To further characterise the precursor relationship of vsRNA-18895, we inspected the strands from which the most abundant vsRNAs derived. The top six vsRNAs (vsRNA-18895, vsRNA-19810, vsRNA-14792, vsRNA-204, vsRNA-711 and vsRNA-29424) all mapped to the same sense strand as NS1/NS2/IV, consistent with processing of these transcripts into a cluster of small RNAs. Critically, the genomic coordinates of these vsRNAs fall entirely within transcript IV, supporting the conclusion that transcript IV serves as the primary precursor for this dominant cluster. Furthermore, because positions 596–615 are also contained in NS1 and NS2, the possibility that NS1 and NS2 also contribute to vsRNA-18895 production cannot be excluded; however, the quantitative dominance of transcript IV-surrounding vsRNAs over those mapping uniquely outside the NS region supports transcript IV as the major producer of vsRNA-18895.

3.4. In Vivo Modulation of vsRNA-18895 Selectively Regulates NS1, NS2 and Transcript IV Expression and Impairs BmBDV Replication

To directly test whether vsRNA-18895 modulates BmBDV gene expression and replication in vivo, we chemically synthesised an agomir (sense strand: 5′-GAAAAGGCUGACG AUCUCCU-3′; antisense strand: 5′-GAGAUCGUCAGCCUUUUCUU-3′) and an antagomir (5′-AGGAGAUCGUCAGCCUUUUC-3′). Because no sensitive BmBDV cell line is available and infection requires an in vivo entry window, fifth-instar larvae were first orally inoculated with BmBDV (5 μL/larva) and then intracoelomically injected with 2 μg/larva of agomir, antagomir, or scrambled negative control (NC) at 8 hpi (Figure 4A). Midguts were sampled at 24, 48, 72 and 96 h post-injection (i.e., 32, 56, 80 and 104 hpi) with three biological replicates per time point. Total RNA and DNA were extracted, and the abundance of each viral transcript (NS1, NS2, IV, VP, PolB, NS3, P133) was quantified by SYBR Green RT-qPCR. Data were normalised to the corresponding NC group at each time point (set to 1).

Strikingly, modulating vsRNA-18895 levels in vivo selectively affected the three transcripts that share its target region. Specifically, agomir treatment increased NS1 expression by $10^{3.52}$-fold (vs. NC) at 24 h post-injection and $10^{2.75}$-fold at 48 h post-injection, whereas antagomir treatment reduced NS1 expression to $10^{-1.87}$-, $10^{-1.92}$-, and $10^{-2.21}$-fold at 24, 48, and 72 h post-injection, respectively (Figure 4B). Similarly, NS2 was induced by $10^{1.71}$-fold at 24 h and $10^{2.47}$-fold at 48 h by agomir, while antagomir reduced NS2 to $10^{-2.77}$-, $10^{-2.16}$-, and $10^{-2.40}$-fold at 24, 48, and 72 h post-injection, respectively (Figure 4C). Likewise, transcript IV was induced $10^{1.87}$-fold by agomir at 24 h post-injection and reduced to $10^{-1.41}$-fold and $10^{-0.94}$-fold at 24 and 48 h post-injection by antagomir, respectively (Figure 4D). By 72–96 h post-injection, no significant differences were detected for any of the three transcripts, consistent with the transient stability of chemically modified oligonucleotides in vivo.

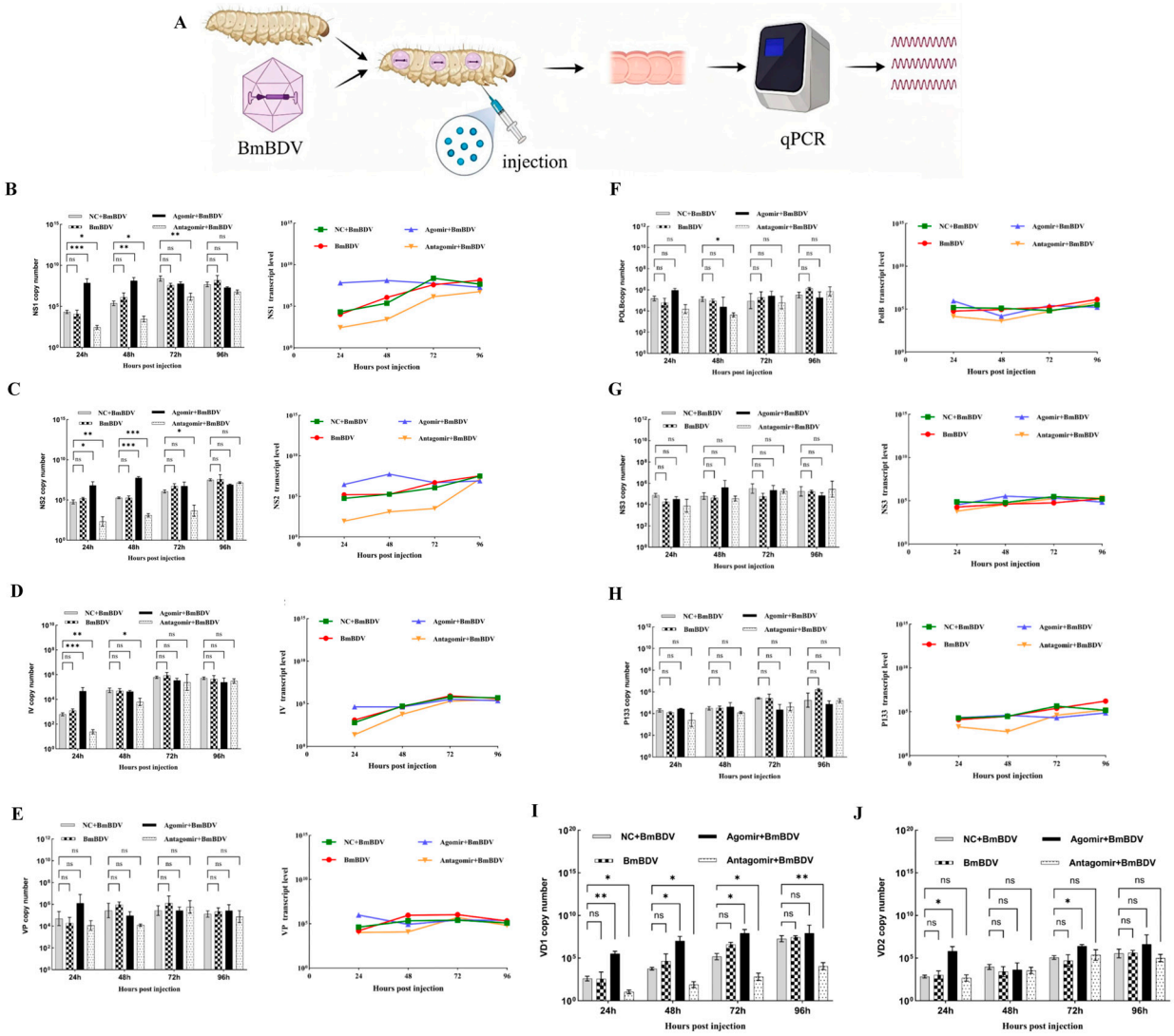


Figure 4. In vivo modulation of vsRNA-18895 selectively regulates NS1, NS2 and IV expression and impairs BmBDV replication. (**A**) Schematic of the agomir/antagomir experimental workflow. Fifth-instar larvae were orally inoculated with BmBDV and intracoelomically injected at 8 hpi with 2 μg/larva of vsRNA-18895 agomir, antagomir, or scrambled negative control (NC). Midguts were sampled at 24, 48, 72 and 96 h post-injection (n = 3 biological replicates/time point). (**B**–**D**) Normalised expression of NS1 (**B**), NS2 (**C**), and transcript IV (**D**) showing selective upregulation by agomir and downregulation by antagomir. (**E**–**H**) Expression of VP (**E**), PolB (**F**), NS3 (**G**) and P133 (**H**) is unaffected by either treatment, confirming selectivity. (**I**,**J**) Absolute copy numbers of viral genomic segments VD1 (**I**) and VD2 (**J**) following agomir/antagomir treatment. NC = scrambled control (set to 1); * $p < 0.05$, ** $p < 0.01$, *** $p < 0.001$, ns $p > 0.05$.

In sharp contrast, VP, PolB, NS3, and P133, which are encoded in regions of the BmBDV genome that lie outside the 596–615 vsRNA-18895 cluster, were largely unaffected by either agomir or antagomir at any of the four time points examined (with the exception of a modest fluctuation of PolB at 48 h) (Figure 4E–H). The NC group did not differ from the BmBDV-only group for any transcript tested ($p > 0.05$), confirming that the observed effects are sequence-specific to vsRNA-18895 rather than to non-specific responses to small RNA injection. Together, these results demonstrate that vsRNA-18895 selectively and positively regulates the three BmBDV transcripts that share its source/predicted target region—NS1, NS2, and transcript IV.

We next asked whether vsRNA-18895 affects BmBDV genome replication. The same experimental samples were used to quantify absolute copy numbers of the viral genomic

segments VD1 and VD2 by qPCR. Compared with the NC group, agomir treatment significantly increased VD1 copy numbers by $10^{2.91}$-, $10^{3.26}$-, and $10^{2.75}$-fold at 24, 48, and 72 h post-injection, respectively, with no significant change at 96 h. Antagomir treatment, in contrast, continuously reduced VD1 copy numbers throughout the time course to $10^{-1.57}$-, $10^{-1.86}$-, $10^{-2.34}$-, and $10^{-3.21}$-fold at 24, 48, 72, and 96 h post-injection, respectively (Figure 4I). For VD2, only a transient induction was observed ($10^{2.99}$-fold at 24 h post-injection by agomir, with no significant changes at later time points), and antagomir had no detectable effect on VD2 at any time point (Figure 4J). Together, these data show that vsRNA-18895 predominantly impacts the replication of the VD1 segment, on which its precursor transcript IV resides.

Taken together, our data support a model in which BmBDV encodes a single "viral non-structural RNA regulon" centred on the NS1/NS2/transcript IV 5′-shared segment: BmBDV produces the novel transcript IV that spans the NS and VP loci of VD1 (290–2929 nt). Within the 5′-shared region of NS1, NS2, and transcript IV lies a vsRNA hotspot dominated by vsRNA-18895 (TPM = 11,750) at positions 596–615 of VD1. In vivo, vsRNA-18895 selectively upregulates the three transcripts that contain its locus—NS1, NS2 and IV—and, through this, promotes VD1 genome replication. Antagomir-mediated knockdown of vsRNA-18895 impairs the expression of these NS transcripts and the replication of the VD1 genome across the entire time course. Thus, the small-RNA hotspot generated from the novel transcript IV engages in a positive feedback loop that coordinates non-structural gene expression and viral replication, with the positive-strand vsRNA-18895 as the most abundant species at this locus.

4. Discussion

In this study, we combined transcriptome sequencing, small RNA sequencing and in vivo gain- and loss-of-function experiments to ask how the transcriptional programme and the small-RNA output of BmBDV are connected during infection of its natural host. The evidence converges on a single regulatory circuit located on the VD1 segment (Figure 5). First, BmBDV expresses a previously unannotated transcript, transcript IV (positions 290–2929 of VD1), that initiates within the TATA-box of the NS1 promoter, terminates at the polyadenylation signal shared with VP, and thus spans the boundary between the non-structural and structural gene loci. Second, the 5′-shared segment of NS1, NS2 and transcript IV contains a small-RNA hotspot dominated by a single 20-nt species, vsRNA-18895 (TPM = 11,750), whose genomic coordinates fall entirely within transcript IV. Third, in vivo modulation of vsRNA-18895 selectively up-regulates NS1, NS2 and transcript IV—the three transcripts that carry its sequence—without affecting the VP, PolB, NS3 or P133 transcripts, and this selectivity translates into a corresponding increase or decrease in replication of the VD1 genome segment. To our knowledge, this is the first evidence in a lepidopteran parvovirus, and indeed in any member of the family Bidnaviridae, that a virus-encoded small RNA acts as a positive regulator of viral transcription and genome replication, and that a viral transcript can simultaneously serve as the precursor of such a regulator.

The identification of transcript IV extends the transcription map of BmBDV and illustrates how compact single-stranded DNA (ssDNA) viruses maximise their limited coding capacity through overlapping transcription units [33]. Parvoviruses are paradigmatic in this respect: in adeno-associated virus, for example, the nested P5, P19 and P40 promoters direct a family of overlapping mRNAs that share 3′ ends and processing signals, allowing distinct protein products to be expressed from a minimal set of cis-acting elements [34]. Insect densoviruses are even more economical, frequently adopting split or ambisense genome organisations in which individual segments carry both non-structural and structural genes [35]. The BmBDV arrangement described here—transcript IV sharing

its transcription start site with NS2 within the TATA-box of the NS1 promoter, and its polyadenylation signal with VP—is a further variant of this shared-element strategy and is fully consistent with the moderately resolved transcription map that we and others had previously deduced by RACE and Northern blotting [36].

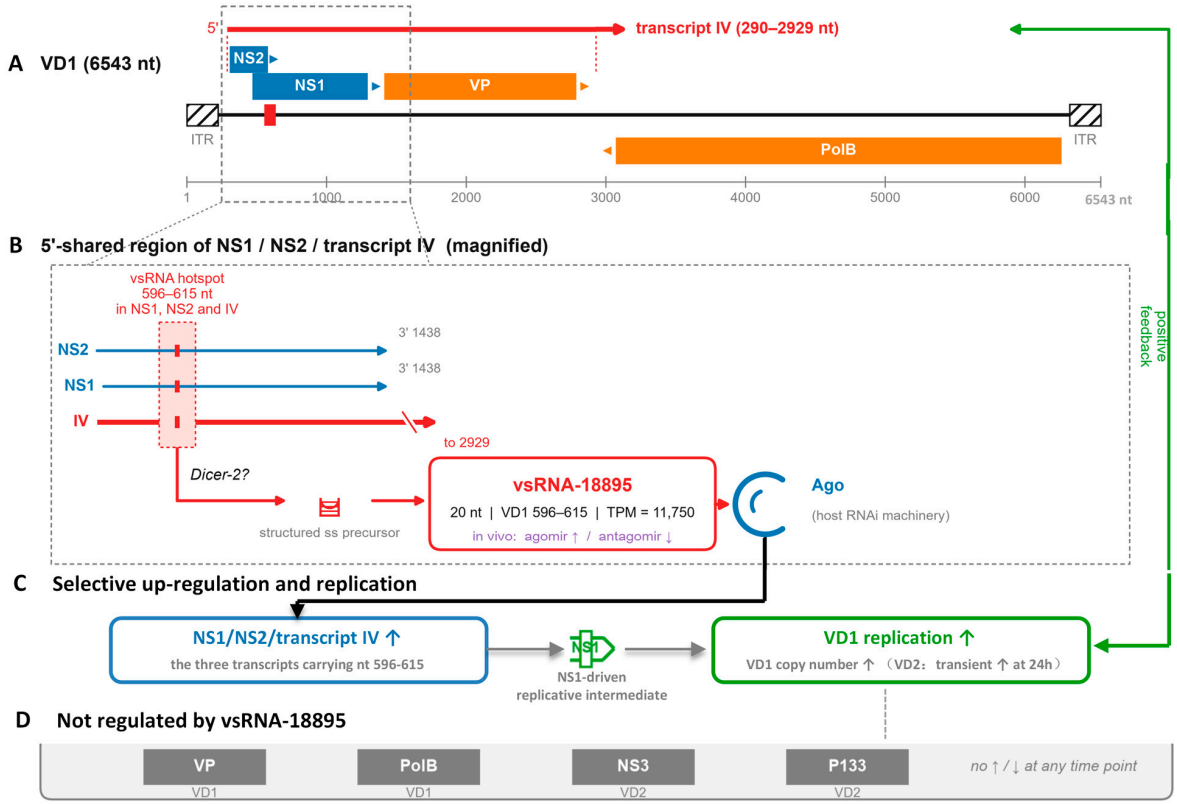


Figure 5. Proposed model of the BmBDV nsRNA regulon. BmBDV transcribes the novel transcript IV (positions 290–2929 of VD1). A vsRNA hotspot within the NS1/NS2/IV-shared 5′ segment produces the dominant vsRNA-18895 (positions 596–615). vsRNA-18895 selectively upregulates NS1, NS2 and IV transcripts, which in turn supports VD1 replication. The NC-only and transcript-unrelated controls (VP, PolB, NS3, P133) confirm selectivity. In the model, grey upward and downward arrows indicate an increase or decrease, respectively, of the transcript or parameter shown; the green arrow denotes the positive-feedback loop that sustains vsRNA-18895 production.

Two properties of transcript IV deserve comment. First, transcript IV was the least abundant VD1-derived transcript at every time point examined, yet its level rose progressively during infection. Low steady-state abundance can reflect either a minor protein-coding mRNA or an RNA whose primary function is regulatory rather than translational. Given that the dominant vsRNA-18895 cluster is nested entirely within the transcribed region of transcript IV, we favour the view that one biologically significant output of transcript IV is the generation of regulatory small RNAs, a possibility that does not exclude a conventional coding function for the same transcript. Second, because BmBDV was long treated as a densovirus and shares the ancestral parvovirus strategy in which several co-terminal transcripts converge on a common non-structural open reading frame [34], transcript IV may also serve as a template for NS1-related translation. Resolving the coding status of transcript IV—for example by ribosome profiling, epitope-tagged overexpression or mass-spectrometry-based proteomics—is an important next step.

The small-RNA population of BmBDV-infected midgut is strongly skewed towards 20–25-nt species, with 20-nt reads alone accounting for nearly half of all viral small RNAs. This size profile is the classic signature of Dicer-dependent processing and is consistent with

the exceptionally active antiviral RNAi pathway of B. mori [20,21]. Comparable processing patterns have been reported for the vsRNA populations of several insect viruses, including a ~20-nt dominant species in a planthopper dicistrovirus [18] and hotspot-like distributions in parvoviruses [16], indicating that small-RNA generation from viral genomes is a general feature of insect virus infections rather than an oddity of BmBDV. In ssDNA viruses, both double-stranded replicative intermediates and folded single-stranded transcripts can act as Dicer substrates [37]; a modest sense-strand bias in the accumulation of the vsRNA-18895 cluster (Figure 3A) is nevertheless consistent with its processing from a structured single-stranded precursor; we note that the near-balanced accumulation of the sense and antisense 20-nt species at this locus does not, however, exclude a substantial contribution from Dicer processing of a transient double-stranded intermediate, which would be expected to yield small RNAs of both polarities [38]. Although we cannot formally exclude contributions from the NS1 and NS2 transcripts, which also contain positions 596–615, three observations point to transcript IV as the principal precursor of the hotspot: its transcribed region spans the entire cluster, the quantitative dominance of the transcript IV-surrounding vsRNAs over species mapping uniquely outside the NS region, and the cluster's confinement to the 5′-shared leader of NS1/NS2/IV. A direct test of this precursor-product relationship, for instance by strand-specific analysis of the pool of transcripts carrying the 596–615 segment or by expressing transcript IV in a heterologous Dicer-competent system, would further consolidate the model.

The most striking functional finding of this work is the direction of regulation. In the best-characterised cases, virus-encoded small RNAs act as repressors: the miRNAs of SV40 and the polyomaviruses, for example, target their own early transcripts and thereby limit T-antigen production [39], and the latency-associated miRNAs of several herpesviruses likewise dampen lytic gene expression [12–14]. vsRNA-18895 acts in the opposite direction—its agomir raises, and its antagomir lowers, the abundance of NS1, NS2 and transcript IV—indicating that this small RNA operates as an activator of its cognate transcriptional unit. Several non-exclusive mechanisms could account for such positive regulation. Small-RNA-mediated gene activation (RNAa) is an established phenomenon in which small RNAs complementary to promoter or 5′ sequences recruit Argonaute complexes and enhance transcription of the corresponding locus [40,41]. Although RNAa was first described in mammalian cells, the functional use of small RNAs to activate gene expression has also been reported in invertebrates, including in the context of viral infection [15,24,42,43]; given that the silkworm Dicer-2/Argonaute-2 antiviral axis is highly active [20,21] and that vsRNA-18895 maps downstream of the shared NS1/NS2/IV transcription start site, it could act through a similar promoter-proximal or antisense-transcript mechanism. Alternatively, in a miRNA-like capacity, vsRNA-18895 could stabilise or translationally enhance the mRNAs that carry its recognition sequence in their 5′ region, an activity documented for a subset of host miRNAs [44] and consistent with the agomir chemistry used here, which is designed to mimic endogenous miRNAs in vivo [45]. A third possibility, unique to the virological context, is that the abundant sense-strand small RNA titrates host RNAi effectors and thereby protects the overlapping viral transcripts from silencing. We therefore propose the testable hypothesis that the 5′ seed of vsRNA-18895 is loaded into an Argonaute complex that is recruited to the shared NS1/NS2/IV promoter and enhances transcriptional initiation in cis. This hypothesis can be examined by (i) strand-specific Argonaute immunoprecipitation or crosslinking from BmBDV-infected midgut to determine whether the sense or the antisense 20-nt species is preferentially loaded into RISC, (ii) mutational inactivation of the 596–615 seed region in a synthetic, replication-competent BmBDV genome, and (iii) direct quantification of vsRNA-18895 and its complementary strand before and after agomir/antagomir injection, which would also establish whether the antagomir acts by reducing small-RNA abundance or by blocking its activity.

A related consideration concerns the complementary antisense small RNA produced from the same locus. At positions 596–615 of VD1, 20-nt small RNAs were detected on both strands at comparable levels (Figure 3A), so it is formally possible that a substantial fraction of the observed effects on the NS1, NS2 and transcript IV levels reflects the action of this antisense species through a conventional RNAi-mediated silencing of the cognate transcripts, or of a Dicer-processed double-stranded intermediate generated at the locus, rather than of the positive-strand molecule alone. The agomir used in this study is a double-stranded oligonucleotide that is itself a substrate for the host RNAi machinery, and the antagomir is expected to enhance antisense-directed silencing; accordingly, our in vivo modulation experiments, which provide association rather than a direct mechanistic proof, cannot at present be attributed unambiguously to the positive-strand vsRNA-18895. We therefore temper the interpretation: the data support a model in which the small-RNA hotspot at the shared 5′ region is functionally coupled to NS1/NS2/IV expression and VD1 replication, but they do not establish that the sense-strand vsRNA-18895 is essential for infection or for the maintenance of NS1/NS2 transcription. A decisive test will require direct measurement of vsRNA-18895 and its complementary species following agomir/antagomir injection, strand-specific Argonaute immunoprecipitation, and mutational inactivation of the 596–615 seed region in a synthetic, replication-competent BmBDV genome; these experiments are underway in our laboratory and will be reported separately.

The selectivity of vsRNA-18895 for the NS1, NS2 and transcript IV unit is biologically coherent with the functions of these gene products. NS1 carries the conserved helicase/ATPase motifs and origin-binding activity that are thought to make it the principal initiator of BmBDV replication [8]; the very rapid elevation of NS1 after agomir treatment, peaking as early as 24 h post-injection, fits an early role in replication and mirrors the temporal expression of NS1 in parvovirus infections [46]. NS2, by contrast, is unrelated to parvovirus NS2 but shares homology with DnaA-like replication-initiation factors, localises to the nuclear envelope, and has been linked to late infection steps such as host–cell lysis and virion release [9]; accordingly, NS2 and transcript IV responded more gradually and remained elevated for longer, echoing the late accumulation of NS2 in BmBDV-infected larvae [9,36]. The observation that only the VD1 segment responds to vsRNA-18895 modulation is likewise consistent with this framework: the NS genes whose expression is controlled by the small RNA reside on VD1, and NS1 is presumably the limiting factor whose supply governs VD1 replication. The transient increase in VD2 copy number observed at 24 h after agomir treatment—in the absence of any significant late-phase change—is intriguing and may reflect an early burst of segment-coordinated replication that later equilibrates, but whether the two segments are replicated and encapsidated under independent or coupled control remains an open question that will require segment-specific reporter systems once a permissive cell line becomes available.

Conceptually, our results place BmBDV on the “proviral” side of the RNAi ledger. In the same silkworm host whose Dicer-2/Argonaute-2 axis constitutes the principal antiviral barrier [20–22], the virus encodes a small RNA that promotes, rather than suppresses, its own gene expression and replication. In this sense BmBDV has co-opted the small-RNA machinery for self-regulation, an evolutionary strategy previously documented mainly among large DNA viruses that encode viral miRNAs to shape latency and immune evasion [12–14], and anticipated for insect viruses by proposals of cis-acting small-RNA regulators [15,24]. That such a strategy has now been demonstrated in the family Bidnaviridae—a lineage that is already exceptional among ssDNA viruses for its bipartite genome and virus-encoded DNA polymerase [47]—reinforces the view that small-RNA-based autoregulation is more widespread among viruses than previously appreciated. On the practical side, the strict coupling between vsRNA-18895 abundance and viral replication suggests that this abundant,

easily detected small RNA could serve as a molecular marker of active BmBDV infection, while the potent antiviral effect of its antagomir provides a proof of principle for sequence-specific RNA-based intervention against a silkworm virus, complementing earlier RNAi and transgenic strategies developed for BmNPV and related pathogens [22,43].

Several limitations of this work should be acknowledged. Both sequencing datasets derive from a single, 72 hpi time point, so the temporal relationship between transcript IV expression, vsRNA-18895 biogenesis and replication could not be resolved dynamically; time-course small-RNA libraries would clarify whether the hotspot accumulates in parallel with transcript IV. The in vivo agomir/antagomir design, necessitated by the absence of a BmBDV-permissive cell line, provides association but not direct proof of mechanism, and the effects waned by 96 h post-injection, consistent with the limited stability of chemically modified oligonucleotides in the larval haemocoel. Whether vsRNA-18895 is processed by Dicer-2 or by an alternative nuclease, which Argonaute protein(s) it engages, and how the positive signal is transmitted to the shared promoter remain to be established. In addition, the functional read-outs reported here are molecular (transcript abundance and genome copy number); we did not assess whether modulating vsRNA-18895 affects larval survival, body weight, development or feeding, nor did we measure the accumulation of complete virus particles, because no BmBDV-permissive cell line, bioassay, or anti-VP antibody is currently available. Extending the analysis to host-level phenotypes and to viral protein levels or titrations will be important for determining whether this regulatory circuit is biologically significant at the whole-organism level, and these experiments are the subject of ongoing work. Finally, the host miRNA response to BmBDV—a rich dataset from the same infected midgut cohort in which eight differentially expressed silkworm miRNAs were identified—is not part of the present manuscript, and integrating the host and viral small-RNA arms will be necessary to understand the full regulatory network. Notwithstanding these caveats, the convergent transcriptomic and functional evidence reported here is consistent with BmBDV using a small RNA generated from a newly identified NS–VP-spanning transcript to sustain a positive feedback loop that couples non-structural gene expression to VD1 replication, although the specific contribution of the positive-strand molecule, as distinct from its complementary species, awaits the mechanistic experiments outlined above. This "transcript → vsRNA → transcriptional activation" module adds a new paradigm to the regulatory biology of insect ssDNA viruses and opens tractable avenues both for mechanistic dissection and for RNA-based control of silkworm densoviral disease.

5. Conclusions

In summary, BmBDV expresses a previously unannotated NS–VP-spanning transcript (transcript IV) whose 5′-shared region with NS1 and NS2 hosts a dominant 20-nt virus-derived small RNA, vsRNA-18895, together with a complementary antisense species of comparable abundance. In vivo agomir/antagomir experiments, which modulate this locus rather than the sense-strand molecule alone, indicate that this small-RNA hotspot is functionally coupled to the expression of NS1, NS2 and transcript IV and to replication of the VD1 segment. We interpret these data as consistent with a virus-encoded small-RNA-mediated positive feedback loop in a lepidopteran parvovirus, while noting that the specific, essential role of the positive-strand vsRNA-18895—as distinct from its complementary strand or a Dicer-processed double-stranded intermediate—remains to be established. This "transcript → vsRNA → transcriptional activation" module nonetheless identifies the 596–615 locus as both a candidate marker of active BmBDV infection and a sequence-specific target for RNA-based control of silkworm disease.

Supplementary Materials: The following supporting information can be downloaded at: https://www.mdpi.com/article/10.3390/insects17111110/s1, Figure S1. Standard curves for the absolute quantification of each BmBDV viral transcript by SYBR Green qPCR. A: NS2; B: NS1; C: VP; D: PolB; E: transcript IV; F: NS3; G: P133. Each panel shows the threshold cycle (Ct) plotted against the copy number of the corresponding standard plasmid (10^0–10^9 copies/μL), with the fitted equation $y = a \cdot \ln(x) + b$ and coefficient of determination (R^2). Figure S2. Length distribution of virus-derived small RNAs (vsRNAs) in the three BmBDV-inoculated midgut libraries (H1, H2, H3). Clean small-RNA reads (15–41 nt) were normalized to reads per million (RPM). The vsRNA population is strongly skewed toward 20–25-nt species, with a dominant 20-nt peak (red dashed line), consistent with Dicer-2-dependent processing. Figure S3. Uncropped RACE gels and Sanger sequencing chromatograms confirming the termini of the novel transcript IV. The agarose gel shows the 5′-RACE and 3′-RACE products of transcript IV, and the chromatograms show the Sanger-sequenced 5′ end (transcription start site, VD1 nt 290) and 3′ end (transcription termination site, VD1 nt 2929). Table S1. The 30 most abundant virus-derived small RNAs (vsRNAs), ranked by total read count. For each vsRNA, the table lists its identifier, sequence, genomic segment (VD1/VD2), position, strand, read counts in the three libraries (H1, H2, H3) and the summed total. Table S2. Oligonucleotide (primer) sequences (5′→3′) used in this study. Stem-loop reverse-transcription (RT) and forward (F) primers for the differentially expressed host miRNAs (bmo-miR-124, bmo-miR-2808a-5p, bmo-miR-2999, bmo-miR-3204a-5p, bmo-miR-6498-3p, bmo-miR-9a-5p, and the novel miRNAs 15 and 34), the U6 snRNA reference, and the universal reverse primer. Table S3. Per-library sequencing statistics for all six transcriptome libraries and three small-RNA libraries (C1–C3 mock-inoculated; H1–H3 BmBDV-inoculated, RNA-seq and sRNA-seq). Columns: sample type, sequencing type, raw and clean read numbers, Q20%, GC% and the percentage of reads aligned to the BmBDV reference.

Author Contributions: Conceptualization, Q.Y.; methodology, J.Y. and Q.Y.; validation, J.Y.; formal analysis, Y.Z.; investigation, J.Y., Y.Z. and Z.X.; resources, Q.Y.; data curation, Y.Z.; writing—original draft preparation, J.Y. and Q.Y.; writing—review and editing, all authors; supervision, Q.Y. and Q.T.; funding acquisition, Q.T. All authors have read and agreed to the published version of the manuscript.

Funding: This research was funded by the National Natural Science Foundation of China, grant number 32673784.

Data Availability Statement: The raw sequencing data generated in this study have been deposited in the NCBI Sequence Read Archive (SRA) under BioProject PRJNA1529325 (BioSample accessions SAMN63138533–SAMN63138538). The deposited data set comprises 15 sequencing runs from six samples and is organised as follows: (i) paired-end transcriptome (RNA-seq) libraries for three BmBDV-inoculated and three mock-inoculated fifth-instar larvae sampled at 72 hpi (six libraries, 12 runs); and (ii) single-end small RNA libraries for the same three BmBDV-inoculated larvae (three libraries, 3 runs). All transcriptome and vsRNA analyses reported in this study were performed on the three BmBDV-inoculated libraries. The BmBDV genome sequences used as mapping references are available in GenBank under accession numbers KX760110 (VD1) and KX779526 (VD2).

Acknowledgments: The authors thank Shanghai Ouyi Medical Technology Biotechnology Co., Ltd. for sequencing services and technical support.

Conflicts of Interest: The authors declare no conflicts of interest. Shanghai Ouyi Medical Technology Biotechnology Co., Ltd. (acknowledged for the sequencing services and technical support described above) had no role in the study design, data analysis, interpretation of the results, or the decision to submit the manuscript, and the authors have no other financial or non-financial relationships with this company that could have influenced the present work.

References

1. Holland, C.; Numata, K.; Rnjak-Kovacina, J.; Seib, F.P. The Biomedical Use of Silk: Past, Present, Future. *Adv. Healthc. Mater.* **2019**, *8*, 1800465. [CrossRef]
2. Yao, Q. The latest nomenclature and classification of silkworm viruses. *Canye Kexue (Sci. Seric.)* **2012**, *33*, 94. (In Chinese)
3. Gomi, S.; Majima, K.; Maeda, S. Sequence analysis of the genome of *Bombyx mori* nucleopolyhedrovirus. *J. Gen. Virol.* **1999**, *80*, 1323–1337. [CrossRef]

4. Bando, H.; Choi, H.; Ito, Y.; Nakagaki, M.; Kawase, S. Structural analysis on the single-stranded genomic DNAs of the virus newly isolated from silkworm: The DNA molecules share a common terminal sequence. *Arch. Virol.* **1992**, *124*, 187–193. [CrossRef]
5. Zhang, X.-L. Study on the Continuous Pathological Changes of Silkworm Infected with *Bombyx mori* Bidensovirus. Master's Thesis, Jiangsu University, Zhenjiang, China, 2016.
6. Wang, Y.J.; Yao, Q.; Chen, K.P.; Wang, Y.; Lu, J.; Han, X. Characterization of the genome structure of *Bombyx mori* densovirus (China isolate). *Virus Genes* **2007**, *35*, 103–108. [CrossRef]
7. Hayakawa, T.; Kojima, K.; Nonaka, K.; Nakagaki, M.; Sahara, K.; Asano, S.-I.; Iizuka, T.; Bando, H. Analysis of proteins encoded in the bipartite genome of a new type of parvo-like virus isolated from silkworm—Structural protein with DNA polymerase motif. *Virus Res.* **2000**, *66*, 101–108. [CrossRef]
8. Li, G.; Sun, C.; Zhang, J.; He, Y.; Chen, H.; Kong, J.; Huang, G.; Chen, K.; Yao, Q. Characterization of *Bombyx mori* parvo-like virus non-structural protein NS1. *Virus Genes* **2009**, *39*, 396–402. [CrossRef]
9. Yu, Q.; Yan, J.; Chen, Y.; Zhang, J.; Tang, Q.; Zhu, F.; Sun, L.; Ma, S.; Liu, X.; Chen, K.; et al. Conserved Nuclear Localization Signal in NS2 Protein of *Bombyx mori* Bidensovirus: A Potential Invertebrate ssDNA Virus Trait. *Viruses* **2025**, *17*, 71. [CrossRef]
10. Li, R.; Chang, P.; Lü, P.; Hu, Z.; Chen, K.; Yao, Q.; Yu, Q. Characterization of the RNA Transcription Profile of *Bombyx mori* Bidensovirus. *Viruses* **2019**, *11*, 325. [CrossRef]
11. Gupta, T.; Raghavendar, G.; Terenius, O.; Ito, K.; Mishra, R.K.; Ponnuvel, K.M. An investigation into the effects of infection and ORF expression patterns of the Indian bidensovirus isolate (*Bm*BDV) infecting the silkworm *Bombyx mori*. *Virus Dis.* **2022**, *33*, 76–83. [CrossRef]
12. Umbach, J.L.; Kramer, M.F.; Jurak, I.; Karnowski, H.W.; Coen, D.M.; Cullen, B.R. MicroRNAs expressed by herpes simplex virus 1 during latent infection regulate viral mRNAs. *Nature* **2008**, *454*, 780–783. [CrossRef]
13. Pfeffer, S.; Zavolan, M.; Grässer, F.A.; Chien, M.; Russo, J.J.; Ju, J.; John, B.; Enright, A.J.; Marks, D.; Sander, C.; et al. Identification of Virus-Encoded MicroRNAs. *Science* **2004**, *304*, 734–736. [CrossRef]
14. Grundhoff, A.; Sullivan, C.S. Virus-encoded microRNAs. *Virology* **2011**, *411*, 325–343. [CrossRef]
15. Ding, S.-W. RNA-based antiviral immunity. *Nat. Rev. Immunol.* **2010**, *10*, 632–644. [CrossRef]
16. Stutika, C.; Mietzsch, M.; Gogol-Döring, A.; Weger, S.; Sohn, M.; Chen, W.; Heilbronn, R. Comprehensive Small RNA-Seq of Adeno-Associated Virus (AAV)-Infected Human Cells Detects Patterns of Novel, Non-Coding AAV RNAs in the Absence of Cellular miRNA Regulation. *PLoS ONE* **2016**, *11*, e0161454. [CrossRef]
17. Wang, Y.; Lin, S.; Zhao, Z.; Xu, P.; Gao, K.; Qian, H.; Zhang, Z.; Guo, X. Functional analysis of a putative *Bombyx mori* cypovirus miRNA BmCPV-miR-10 and its effect on virus replication. *Insect Mol. Biol.* **2021**, *30*, 552–565. [CrossRef]
18. Li, J.; Andika, I.B.; Zhou, Y.; Shen, J.; Sun, Z.; Wang, X.; Sun, L.; Chen, J. Unusual characteristics of dicistrovirus-derived small RNAs in the small brown planthopper, *Laodelphax striatellus*. *J. Gen. Virol.* **2014**, *95*, 712–718. [CrossRef]
19. Monsanto-Hearne, V.; Johnson, K.N. miRNA Modulation of Insect Virus Replication. *Curr. Issues Mol. Biol.* **2020**, *34*, 61–82. [CrossRef]
20. Zhu, K.Y.; Palli, S.R. Mechanisms, Applications, and Challenges of Insect RNA Interference. *Annu. Rev. Entomol.* **2020**, *65*, 293–311. [CrossRef]
21. Wang, X.-H.; Aliyari, R.; Li, W.-X.; Li, H.-W.; Kim, K.; Carthew, R.; Atkinson, P.; Ding, S.-W. RNA Interference Directs Innate Immunity Against Viruses in Adult *Drosophila*. *Science* **2006**, *312*, 452–454. [CrossRef]
22. Santos, D.; Wynant, N.; Van den Brande, S.; Verdonckt, T.-W.; Mingels, L.; Peeters, P.; Kolliopoulou, A.; Swevers, L.; Vanden Broeck, J. Insights into RNAi-based antiviral immunity in Lepidoptera: Acute and persistent infections in *Bombyx mori* and *Trichoplusia ni* cell lines. *Sci. Rep.* **2018**, *8*, 2423. [CrossRef]
23. Bartel, D.P. MicroRNAs: Target Recognition and Regulatory Functions. *Cell* **2009**, *136*, 215–233. [CrossRef]
24. Hussain, M.; Asgari, S. MicroRNA-like viral small RNA from Dengue virus 2 autoregulates its replication in mosquito cells. *Proc. Natl. Acad. Sci. USA* **2014**, *111*, 2746–2751. [CrossRef]
25. Andrews, S. FastQC: A Quality Control Tool for High Throughput Sequence Data. 2010. Available online: http://www.bioinformatics.babraham.ac.uk/projects/fastqc/ (accessed on 17 September 2026).
26. Bolger, A.M.; Lohse, M.; Usadel, B. Trimmomatic: A flexible trimmer for Illumina sequence data. *Bioinformatics* **2014**, *30*, 2114–2120. [CrossRef]
27. Dobin, A.; Davis, C.A.; Schlesinger, F.; Drenkow, J.; Zaleski, C.; Jha, S.; Batut, P.; Chaisson, M.; Gingeras, T.R. STAR: Ultrafast universal RNA-seq aligner. *Bioinformatics* **2013**, *29*, 15–21. [CrossRef]
28. Pertea, M.; Pertea, G.M.; Antonescu, C.M.; Chang, T.-C.; Mendell, J.T.; Salzberg, S.L. StringTie enables improved reconstruction of a transcriptome from RNA-seq reads. *Nat. Biotechnol.* **2015**, *33*, 290–295. [CrossRef]
29. Haas, B.J. TransDecoder (Find Open Reading Frames in Transcripts). Available online: https://github.com/TransDecoder/TransDecoder (accessed on 17 September 2026).
30. Li, B.; Dewey, C.N. RSEM: Accurate transcript quantification from RNA-Seq data with or without a reference genome. *BMC Bioinform.* **2011**, *12*, 323. [CrossRef]

31. Langmead, B.; Trapnell, C.; Pop, M.; Salzberg, S.L. Ultrafast and memory-efficient alignment of short DNA sequences to the human genome. *Genome Biol*. **2009**, *10*, R25. [CrossRef]
32. Bustin, S.A.; Benes, V.; Garson, J.A.; Hellemans, J.; Huggett, J.; Kubista, M.; Mueller, R.; Nolan, T.; Pfaffl, M.W.; Shipley, G.L.; et al. The MIQE Guidelines: Minimum Information for Publication of Quantitative Real-Time PCR Experiments. *Clin*. *Chem*. **2009**, *55*, 611–622. [CrossRef]
33. Cotmore, S.F.; Agbandje-McKenna, M.; Chiorini, J.A.; Mukha, D.V.; Pintel, D.J.; Qiu, J.; Soderlund-Venermo, M.; Tattersall, P.; Tijssen, P.; Gatherer, D.; et al. The family Parvoviridae. *Arch*. *Virol*. **2014**, *159*, 1239–1247. [CrossRef]
34. Kyöstiö, S.R.; Owens, R.A.; Weitzman, M.D.; Antoni, B.A.; Chejanovsky, N.; Carter, B.J. Analysis of adeno-associated virus (AAV) wild-type and mutant Rep proteins for their abilities to negatively regulate AAV p5 and p19 mRNA levels. *J*. *Virol*. **1994**, *68*, 2947–2957. [CrossRef]
35. Baquerizo-Audiot, E.; Abd-Alla, A.; Jousset, F.-X.; Cousserans, F.; Tijssen, P.; Bergoin, M. Structure and Expression Strategy of the Genome of *Culex pipiens* Densovirus, a Mosquito Densovirus with an Ambisense Organization. *J*. *Virol*. **2009**, *83*, 6863–6873. [CrossRef]
36. Yu, Q.; Tijssen, P. Gene Expression of Five Different Iteradensoviruses: *Bombyx mori* Densovirus, *Casphalia extranea* Densovirus, *Papilio polyxenes* Densovirus, *Sibine fusca* Densovirus, and *Danaus plexippus* Densovirus. *J*. *Virol*. **2014**, *88*, 12152–12157. [CrossRef]
37. Hayakawa, T.; Asano, S.; Sahara, K.; Iizuka, T.; Bando, H. Detection of replicative intermediate with closed terminus of *Bombyx* densonucleosis virus. *Arch*. *Virol*. **1997**, *142*, 393–399. [CrossRef]
38. Schwarz, D.S.; Hutvágner, G.; Du, T.; Xu, Z.; Aronin, N.; Zamore, P.D. Asymmetry in the Assembly of the RNAi Enzyme Complex. *Cell* **2003**, *115*, 199–208. [CrossRef]
39. Sullivan, C.S.; Grundhoff, A.T.; Tevethia, S.; Pipas, J.M.; Ganem, D. SV40-encoded microRNAs regulate viral gene expression and reduce susceptibility to cytotoxic T cells. *Nature* **2005**, *435*, 682–686. [CrossRef]
40. Li, L.-C.; Okino, S.T.; Zhao, H.; Pookot, D.; Place, R.F.; Urakami, S.; Enokida, H.; Dahiya, R. Small dsRNAs induce transcriptional activation in human cells. *Proc*. *Natl*. *Acad*. *Sci*. *USA* **2006**, *103*, 17337–17342. [CrossRef]
41. Janowski, B.A.; Younger, S.T.; Hardy, D.B.; Ram, R.; Huffman, K.E.; Corey, D.R. Activating gene expression in mammalian cells with promoter-targeted duplex RNAs. *Nat*. *Chem*. *Biol*. **2007**, *3*, 166–173. [CrossRef]
42. Zhao, W.; Li, Q.; Sun, M.; Luo, L.; Zhang, X.; Cui, F. Small interfering RNAs generated from the terminal panhandle structure of negative-strand RNA virus promote viral infection. *PLoS Pathog*. **2025**, *21*, e1012789. [CrossRef]
43. Jiang, L.; Zhao, P.; Cheng, T.; Sun, Q.; Peng, Z.; Dang, Y.; Wu, X.; Wang, G.; Jin, S.; Lin, P.; et al. A transgenic animal with antiviral properties that might inhibit multiple stages of infection. *Antivir*. *Res*. **2013**, *98*, 171–173. [CrossRef]
44. Vasudevan, S.; Tong, Y.; Steitz, J.A. Switching from Repression to Activation: MicroRNAs Can Up-Regulate Translation. *Science* **2007**, *318*, 1931–1934. [CrossRef]
45. Li, P.; Gao, Y.; Zhou, R.; Che, X.; Wang, H.; Cong, L.; Jiang, P.; Liang, D.; Li, P.; Wang, C.; et al. Intra-articular injection of miRNA-1 agomir, a novel chemically modified miRNA agonists alleviates osteoarthritis (OA) progression by downregulating Indian hedgehog in rats. *Sci*. *Rep*. **2024**, *14*, 8101. [CrossRef]
46. Deleu, L.; Pujol, A.; Faisst, S.; Rommelaere, J. Activation of Promoter P4 of the Autonomous Parvovirus Minute Virus of Mice at Early S Phase Is Required for Productive Infection. *J*. *Virol*. **1999**, *73*, 3877–3885. [CrossRef]
47. Krupovic, M.; Koonin, E.V. Evolution of eukaryotic single-stranded DNA viruses of the *Bidnaviridae* family from genes of four other groups of widely different viruses. *Sci*. *Rep*. **2014**, *4*, 5347. [CrossRef]

Disclaimer/Publisher's Note: The statements, opinions and data contained in all publications are solely those of the individual author(s) and contributor(s) and not of MDPI and/or the editor(s). MDPI and/or the editor(s) disclaim responsibility for any injury to people or property resulting from any ideas, methods, instructions or products referred to in the content.